The preparation of Ph_3PAu carboxylates is relatively simple compared to that of other organogold(I) complexes. The preparation of the Ph_3PAu(carboxylate) can be done in the presence of air and moisture. In addition, formation of a gold film occurs at lower temperatures than in conventional CVD methods.

(12) Kodas, T. T.; Baum, T. H.; Comita, P. B. *J. Appl. Phys.* **1987**, *62* (1), 281.
(13) Baum, T. H. *J. Electrochem. Soc.: Solid State Sci. Technol.* **1987**, *134* (10), 2616.

Acknowledgment. This work has been supported by the National Science Foundation, the Robert A. Welch Foundation, and the Texas Engineering Experiment Station. We thank Steve P. Chum, Dow Chemical Co., for suggesting the problem.

Supplementary Material Available: Full tables of anisotropic thermal parameters and hydrogen atom coordinates for the two compounds reported (5 pages); listings of structure factors (33 pages). Ordering information is given on any current masthead page.

Reactions of $(\eta\text{-}C_5Me_5)Ta(PMe_3)(H)_2(\eta^2\text{-}CHPMe_2)$ and the Nature of the $\eta^2\text{-}CHPMe_2$ Ligand

H. Mary Anstice,[1a] Helen H. Fielding,[1a] Vernon C. Gibson,*[,1b] Catherine E. Housecroft,*[,1a] and Terence P. Kee[1b,c]

Department of Chemistry, University Science Laboratories, South Road, Durham DH1 3LE, U.K., and University Chemical Laboratory, Lensfield Road, Cambridge CB2 1EW, U.K.

Received October 4, 1990

Treatment of $(\eta\text{-}C_5Me_5)Ta(PMe_3)(H)_2(\eta^2\text{-}CHPMe_2)$ (1) with tertiary phosphines and phosphites leads to an equilibrium mixture of 1 and $(\eta\text{-}C_5Me_5)Ta(PR_3)(H)_2(\eta^2\text{-}CHPMe_2)$ (**3a–d**). Equilibrium constants, determined in benzene, are less than unity and decrease in the order $PMe_2Ph \approx P(OMe)_3 > PEt_3 > PMePh_2 > P(OPh)_3$. 1 reacts with dmpe to give the adduct $(\eta\text{-}C_5Me_5)Ta(\eta^1\text{-dmpe})(H)_2(\eta^2\text{-}CHPMe_2)$ (4) followed by $(\eta\text{-}C_5Me_5)Ta(dmpe)(H)(\eta^2\text{-}CH_2PMe_2)$ (5) arising by a metal → carbon hydrogen migration. Carbon monoxide reacts with 1 to give a mixture of $(\eta\text{-}C_5Me_5)Ta(CO)_2(PMe_3)_2$ (6) and $(\eta\text{-}C_5Me_5)Ta(CO)_3(PMe_3)$ (7), while dihydrogen reacts to give $(\eta\text{-}C_5Me_5)Ta(PMe_3)_2H_4$ (8). Treatment of 1 with 1 equiv of MeX (X = Cl, Br, I) affords $(\eta\text{-}C_5Me_5)Ta(PMe_3)(H)(X)(\eta^2\text{-}CHPMe_2)$ (**9a–c**) and treatment with excess MeX, $(\eta\text{-}C_5Me_5)Ta(X)_2(\eta^2\text{-}CHPMe_2)$ (**11a–c**). A comparison of the bonding in $(\eta\text{-}C_5Me_5)NbCl_2(\eta^2\text{-}CHPMe_2)$ with that in $(\eta\text{-}C_5Me_5)NbCl_2(HC{\equiv}CH)$ using Fenske–Hall quantum chemical calculations suggests that the $\eta^2\text{-}CHPMe_2$ ligand is best described as a phosphinocarbene rather than a phosphaalkyne.

Introduction

We have recently shown that $(C_5Me_5)Ta(PMe_3)_2$ exists in the two unusual cyclometalated forms 1 and 2, which

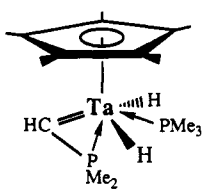

(1)

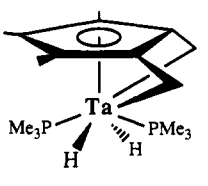

(2)

do not readily interconvert.[2c] A potentially useful feature of these compounds is the retention of the abstracted hydrogens within the metal coordination sphere allowing an opportunity to exploit the reverse metal → carbon hydrogen migrations to generate coordinatively unsaturated, highly reactive tantalum species.

This paper presents the results of some of our investigations into the first of these isomers, the phosphine-metalated form 1. We were particularly interested to establish the viability of the reverse hydrogen migrations to give first $[Ta(H)(\eta^2\text{-}CH_2PMe_2)]$ and thence regenerate the classical PMe_3 ligand (eq 1) and also to explore the de-

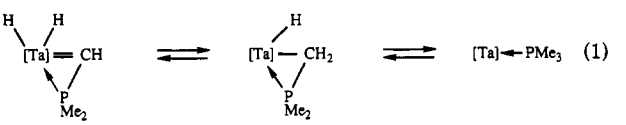

(1)

rivative chemistry of 1 in which the $\eta^2\text{-}CHPMe_2$ ligand is retained. Fenske–Hall quantum chemical calculations have been employed to probe the nature of the 4-electron $(\eta^2\text{-}CHPMe_2)$ ligand and allow a comparison with 4-electron acetylene ligands.

Results and Discussion

1. Reactions of 1 with Tertiary Phosphines and Phosphites. 1 reacts with phosphines and phosphites by displacement of the PMe_3 ligand to give adducts of the type $(\eta\text{-}C_5Me_5)Ta(PR_3)(H)_2(\eta^2\text{-}CHPMe_2)$ (Scheme I). The adducts are readily characterized by ^1H NMR spectroscopy (Table I) but have not been isolated. Equilibrium was reached within 6 days at room temperature, and there was no evidence for the formation of $Cp^*Ta(H)(\eta^2\text{-}CH_2PMe_2)(PR_3)_2$ or $Cp^*Ta(PMe_3)_2(PR_3)_2$. The equilibrium mixture is stable over several months at room temperature for the tertiary phosphine derivatives, but with

(1) (a) University of Cambridge. (b) University of Durham. (c) Present address: School of Chemistry, University of Leeds, Leeds, LS2 9JT, U.K.
(2) (a) Kee, T. P.; Gibson, V. C.; Clegg, W. *J. Organomet. Chem.* **1987**, *325*, C14. (b) Carter, S. T.; Clegg, W.; Gibson, V. C.; Kee, T. P.; Sanner, R. D. *Organometallics* **1989**, *8*, 253. (c) Carter, S. T.; Clegg, W.; Gibson, V. C.; Kee, T. P.; Sanner, R. D. Manuscript in preparation.

0276-7333/91/2310-2183$02.50/0

Table I. NMR Data

compd	assgnt	chem shifts (ppm), multiplicity, coupling consts (Hz)		
		^{1}H	^{13}C	^{31}P
Cp*Ta(PR_3)(H)$_2$-(η^2-CHPMe_2)				
R_3 = Me_2Ph (**3a**)	C*H*PMe_2	9.23, t, ^2J(PH) = 2.7		
	C_6H_5	7.1–7.5, m		
	Ta–*H*	4.14, dd, ^2J(PH) = 53.0, 18.0		
	$C_5(CH_3)_5$	2.06, s		
	P*Me*$_2$Ph	1.75, d, ^2J(PH) = 6.4		
	CHP*Me*$_2$	1.33, d, ^2J(PH) = 10.4		
R_3 = Et_3 (**3b**)[a]	C*H*PMe_2	9.22, t, ^2J(PH) = 2.9		
	Ta–*H*	3.75, dd, ^2J(PH) = 51.8, 18.0		
	$C_5(CH_3)_5$	2.18, s		
	CHP*Me*$_2$	1.39, d, ^2J(PH) = 11.8		
R_3 = $MePh_2$ (**3c**)[a]	C*H*PMe_2	9.39, t, ^2J(PH) = 2.4		
	Ta–*H*	4.48, dd, ^2J(PH) = 56.3, 18.3		
	$C_5(CH_3)_5$	2.07, s		
	CHP*Me*$_2$	1.15, d, ^2J(PH) = 10.0		
R_3 = $(OMe)_3$ (**3d**)[b]	C*H*PMe_2	9.08, t, ^2J(PH) = 2.9		
	P(O*Me*)$_3$	3.42, d, ^3J(PH) = 9.6		
	$C_5(CH_3)_5$	2.27, s		
	CHP*Me*$_2$	1.43, d, ^2J(PH) = 11.7		
Cp*Ta(dmpe)(H)$_2$-(η^2-CHPMe_2) (**4**)[c]	C*H*PMe_2	9.18, t, ^2J(PH) = 2.8		
	Ta–*H*	3.75, dd, ^2J(PH) = 53.5, 17.7		
	$C_5(CH_3)_5$	2.18, s		
Cp*Ta(dmpe)(H)-(η^2-CH_2PMe_2) (**5**)	$C_5(CH_3)_5$	2.27, s		
	P$_C$*Me*^{2}	1.84, d, ^2J(P$_C$H) = 9.0		
	P$_C$*Me*^{1}	1.44, d, ^2J(P$_C$H) = 7.6		
	P$_B$*Me*^{6}	1.52, d, ^2J(P$_B$H) = 7.8		
	P$_B$*Me*^{4}	1.22, d, ^2J(P$_B$H) = 5.1		
	P$_A$*Me*^{3}	1.14, d, ^2J(P$_A$H) = 4.9		
	P$_A$*Me*^{5}	0.92, d, ^2J(P$_A$H) = 5.5		
	PCH_2CH_2P	1.33, m		
	H^3	0.26, ddddd, ^3J(P$_A$H) = 8.0, ^3J(P$_B$H) = 15.8, ^3J(P$_C$H) = 6.4, ^3J(H^{1}H^3) = 5.3, ^2J(H^{2}H^3) = 8.0		
	H^2	−0.97, ddddd, ^3J(P$_A$H) = 8.4, ^3J(P$_B$H) = 23.9, ^3J(P$_C$H) = 3.0, ^3J(H^{1}H^2) = 2.3, ^2J(H^{3}H^2) = 8.0		
	H^1	−2.96, ddddd, ^2J(P$_A$H) = 28.0, ^2J(P$_B$H) = 6.5, ^2J(P$_C$H) = 15.0, ^3J(H^{2}H^1) = 2.3, ^3J(H^{3}H^1) = 5.3		
	$C_5(CH_3)_5$		14.3, s	
	$C_5(CH_3)_5$		96.4, s	
	P(CH_3)		26.8, d, ^1J(PC) = 32.0	
			26.7, d, ^1J(PC) = 32.0	
			25.6, d, ^1J(PC) = 20.1	
			19.2, d, ^1J(PC) = 11.7	
			18.6, m	
			16.6, d, ^1J(PC) = 14.0	
	PCH_2CH_2P		37.2, dd, ^1J(PC) = 25.8, ^2J(PC) = 13.3	
			33.1, dd, ^1J(PC) = 23.1, ^2J(PC) = 12.1	
	P$_A$			25.6, dd, J(P$_A$P$_B$) = 38.8, J(P$_A$P$_C$) = 18.6
	P$_B$			21.5, dd, J(P$_A$P$_B$) = 38.8, J(P$_B$P$_C$) = 10.3
	P$_C$			−53.6, dd, J(P$_A$P$_C$) = 18.6, J(P$_B$P$_C$) = 10.3
Cp*Ta(PMe_3)(H)(Br)-(η^2-CHPMe_2) (**9a**)	C*H*PMe_2	9.22, s (not resolved)		
	Ta–*H*	5.66, dd, ^2J(PH) = 47.5, 25.0		
	$C_5(CH_3)_5$	2.09, s		
	P*Me*$_2$	1.52, d, ^2J(PH) = 11.0		
	P*Me*$_2$	1.46, d, ^2J(PH) = 10.6		
	P*Me*$_3$	1.32, d, ^2J(PH) = 7.0		
	C*H*PMe_2		196.7, d, ^1J(PC) = 48.7	
	$C_5(CH_3)_5$		111.2, s	
	P(CH_3)$_3$		18.9, d, ^1J(PC) = 14.7	
	$C_5(CH_3)_5$		12.6, s	
	P(CH_3)$_2$[d]		11.3, d, ^1J(PC) = 24.2	
	PMe_2			−104.2, d, ^2J(PP) = 47.7
	PMe_3			−33.2, d, ^2J(PP) = 47.7
Cp*Ta(PMe_3)(H)(I)-(η^2-CHPMe_2) (**9b**)	C*H*PMe_2	9.53, s (not resolved)		
	Ta–*H*	4.08, dd, ^2J(PH) = 51.4, 28.0		
	$C_5(CH_3)_5$	2.07, s		
	P*Me*$_2$	1.68, d, ^2J(PH) = 10.8		
	P*Me*$_2$	1.40, d, ^2J(PH) = 10.2		
	P*Me*$_3$	1.42, d, ^2J(PH) = 6.8		

Table I (Continued)

compd	assgnt	chem shifts (ppm), multiplicity, coupling consts (Hz)		
		^1H	^{13}C	^{31}P
Cp*Ta(PMe_3)(H)(I)-(η^2-CHPMe_2) (**9b**)	$CHPMe_2$		202.1, d, ^1J(PC) = 50.1	
	$C_5(CH_3)_5$		110.7, s	
	$P(CH_3)_3$		20.6, d, ^1J(PC) = 19.9	
	$C_5(CH_3)_5$		13.2, s	
	$P(CH_3)_2$		19.5, d, ^1J(PC) = 28.7	
			13.6, d, ^1J(PC) = 24.3	
	PMe_2			-107.8, d, ^2J(PP) = 46.1
	PMe_3			-41.0, d, ^2J(PP) = 46.1
Cp*Ta(PMe_3)(H)(Cl)-(η^2-CHPMe_2) (**9c**)	$CHPMe_2$	9.00, s (not resolved)		
	Ta-*H*	6.73, dd, ^2J(PH) = 44.6, 26.3		
	$C_5(CH_3)_5$	2.03, s		
	PMe_2	1.45, d, ^2J(PH) = 10.6		
	PMe_2	1.42, d, ^2J(PH) = 10.8		
	PMe_3	1.27, d, ^2J(PH) = 6.1		
Cp*$TaCl_2$(η^2-CHPMe_2) (**11a**)	$CHPMe_2$	9.92, s (not resolved)		
	$C_5(CH_3)_5$	1.87, s		
	PMe_2	1.52, d, ^2J(PH) = 11.1		
Cp*$TaBr_2$(η^2-CHPMe_2) (**11b**)	$CHPMe_2$	10.49, s (not resolved)		
	$C_5(CH_3)_5$	1.90, s		
	PMe_2	1.62, d, ^2J(PH) = 11.3		
	$CHPMe_2$		207.1, d, ^1J(PC) = 48.1	
	$C_5(CH_3)_5$		118.4, s	
	$C_5(CH_3)_5$		12.1, s	
	$P(CH_3)_2$[e]		12.4, d, ^1J(PC) ≈ 20	
	PMe_2			-28.4 s
Cp*TaI_2(η^2hCHPMe_2) (**11c**)	$CHPMe_2$	11.28, s (not resolved)		
	$C_5(CH_3)_5$	1.99, s		
	PMe_2	1.80, d, ^2J(PH) = 11.3		
	$CHPMe_2$		not found	
	$C_5(CH_3)_5$		97.8, s	
	$C_5(CH_3)_5$		13.9, s	
	$P(CH_3)_2$		16.2, d, ^1J(PC) = 30.0	
	PMe_2			-37.6, s

[a] Signals for the PR_3 ligand could not be assigned unambiguously due to signal overlap. [b] Hydride signal not located. [c] The methyl hydrogens of $CHPMe_2$ and dmpe and the dmpe methylene hydrogens could not be identified unambiguously due to extensive signal overlap. [d] Only one PMe_2 carbon is resolved; the other is obscured by the signal at 18.9 ppm. [e] The PMe_2 carbon resonance is partially obscured by the methyl carbons of the Cp* ligand.

Scheme I

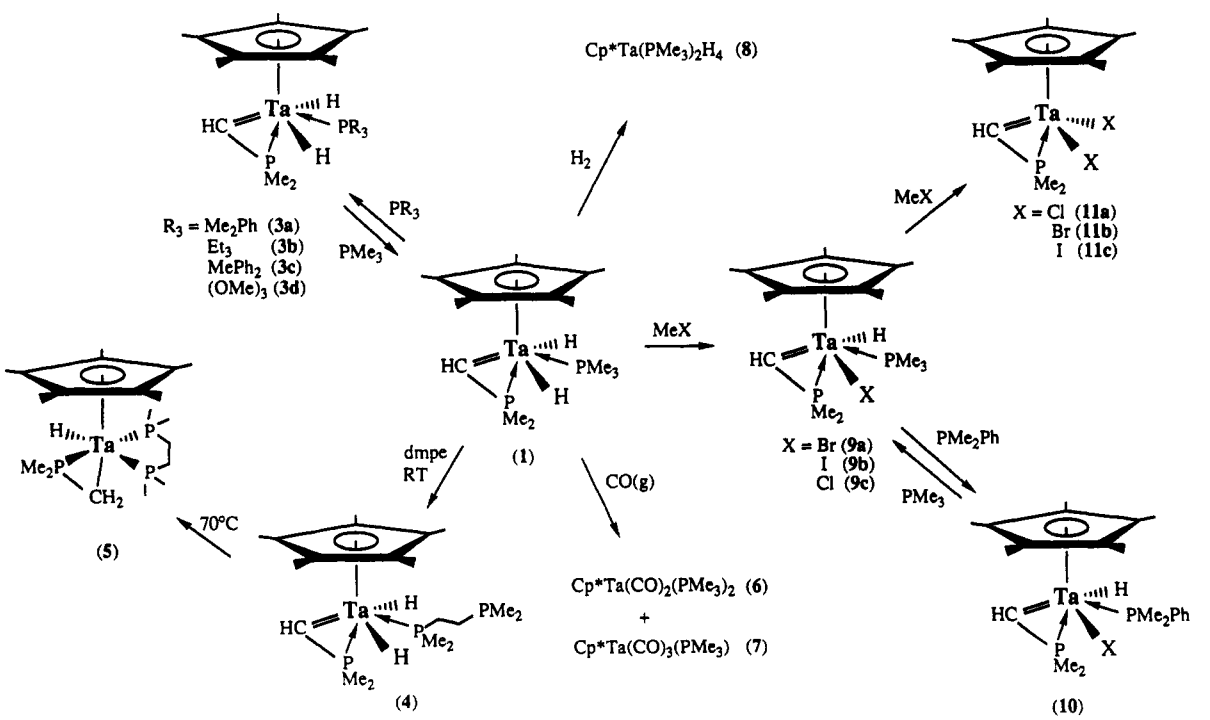

$P(OMe)_3$ decomposition to undefined products occurs within 3–4 weeks at 25 °C.

The equilibrium constants (K_p), calculated in benzene-d_6 at 298 K, are collected in Table II, along with values of ν and θ as a measure of the electronic and steric properties of the PR_3 ligands.[3] The order of decreasing K_p is found to be PMe_3 > PMe_2Ph ≈ $P(OMe)_3$ > PEt_3 > $PMePh_2$ > $P(OPh)_3$, which is at variance with the order predicted on the basis of steric requirements alone (i.e. $P(OMe)_3$ > PMe_3 > PMe_2Ph > $P(OPh)_3$ > PEt_3 > $PMePh_2$). The two

Table II. Equilibrium Constants for Phosphine and Phosphite Exchange with PMe_3 in 1

ligand	K_p[a]	ν, cm^{-1}	θ, deg
PMe_3	1.0	2064.1	118
PMe_2Ph	1.50 (5) × 10^{-1}	2065.3	122
$PMePh_2$	1.8 (3) × 10^{-3}	2067.0	136
PEt_3	2.0 (3) × 10^{-2}	2061.7	132
$P(OMe)_3$	1.47 (7) × 10^{-1}	2079.5	107
$P(OPh)_3$	*b*	2085.3	128

[a] Determined in benzene-d_6 at 298 K (mean of three determinations). [b] Too small to measure under the conditions employed.

phosphite adducts have significantly lower K_p values than expected, presumably due to an overriding electronic factor; the Ta(V) metal center in **1** may be regarded as a hard acid and consequently is expected to be stabilized most favorably by a hard, electron-releasing base.[4] Since the ν parameters are a measure of the basicity of the phosphorus ligands, we would expect the phosphite ligands to possess the lower K_p values.

2. Reaction of 1 with Bis(dimethylphosphino)ethane (dmpe). Although tertiary monophosphines participate in ligand-exchange equilibria with **1**, they do not lead to trapping of intermediates arising from tantalum-to-carbon hydrogen migrations. We envisaged that a chelating disphosphine would be better able to stabilize the $[M(H)(\eta^2\text{-}CH_2PMe_2)]$ moiety toward swift regeneration of $[M(H)_2(\eta^2\text{-}CHPMe_2)]$, since a vacant site is required for such a process and the chelating phosphine is less labile than its monophosphine counterparts. **1** reacts smoothly with 1 molar equiv of dmpe at 70 °C to give an intermediate adduct **4** in which one end only of the dmpe ligand is bound to the metal, followed by conversion to the chelate complex **5** (Scheme I).

4 has not been isolated but is readily identified by comparison of its ^1H NMR spectrum, obtained on a reaction mixture maintained at room temperature, with those of the phosphine adducts **3a–d**. Although it has not proved possible to locate all of the dmpe ligand hydrogens, the NMR data are consistent with a structure analogous to that of compounds **1** and **3a–d**, in which PMe_3 has been displaced by dmpe bound through only one of its two PMe_2 units. **5** can be envisaged to result from the trapping of $[Cp^*Ta(\eta^1\text{-dmpe})(H)(\eta^2\text{-}CH_2PMe_2)]$, providing further confirmation that hydrogen migrations do indeed occur on the time scale of a chemical reaction. Characteristic shifts in the ^1H, ^{31}P, and ^{13}C NMR spectra (Table I) confirm the presence of the $\eta^2\text{-}CH_2PMe_2$ ligand: in particular, the phosphorus nucleus resonates at −53.6 ppm, while a signal 4.12 ppm in the ^{13}C NMR spectrum is attributable to the methylene carbon. These shifts are quite different from those observed for the metallacycle carbon and phosphorus nuclei in the $[Ta(\eta^2\text{-}CHPMe_2]$ moiety[2a,c,5] (typically −112 to −140 ppm (^{31}P) and 170–194 ppm (^{13}C), respectively). The single hydride ligand is observed at −2.96 ppm in the ^1H NMR spectrum, which also shows six distinct doublets between 1.84 and 1.92 ppm attributable to the phosphorus methyl substituents. The inequivalence of all the P-methyls is consistent with a number of ligand arrangements and orientations around the metal. However, difference nOe experiments suggest that the preferred geometry is that in which the three phosphorus atoms and the hydride occupy a pseudoequatorial plane leaving the methylene of the metallacycle to occupy a site trans to the Cp* ligand:

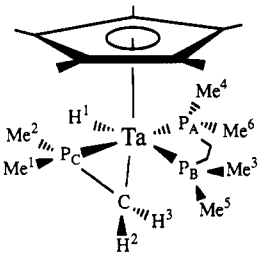

For example, irradiation of the Cp* ring hydrogens results in an enhancement of the metal hydride resonance (ca. 7%) and one methyl group on each dmpe phosphorus atom (ca. 3% each). There is also enhancement (ca. 3%) of both methyls attached to the phosphorus of the metallacycle but no detectable effect upon the methylene hydrogens, suggesting that the $\eta^2\text{-}CH_2PMe_2$ ligand is oriented with the PMe_2 terminus nearest to the Cp* ring. ^1H–^1H and selective ^{31}P–^1H decoupling experiments have facilitated an assignment of all the phosphorus methyl resonances and the couplings observed in the hydride and CH_2PMe_2 methylene signals. Finally, irradiation of the methylene hydrogen resonance at 0.26 ppm results in a nuclear Overhauser enhancement to Ta–*H* (ca. 4%), while irradiation of its diastereotopic partner at −0.97 ppm has no effect on the hydride resonance. Thus, the 0.26 ppm signal may be attributed to H_3, which lies on the same side of the molecule as the hydride ligand.

3. Reactions of 1 with Carbon Monoxide and Dihydrogen. **1** reacts slowly with CO(g) (1 atm) at room temperature to give a mixture of *cis*- and *trans*-$Cp^*Ta(CO)_2(PMe_3)_2$ (**6**, 70%) and $Cp^*Ta(CO)_3(PMe_3)$ (**7**, 30%) by ^1H NMR spectroscopy. Both **6** and **7** have been characterized previously.[6] Their proportions in the reaction mixture are dependent upon the temperature of the reaction, the pressure of CO employed, and the reaction

Scheme II

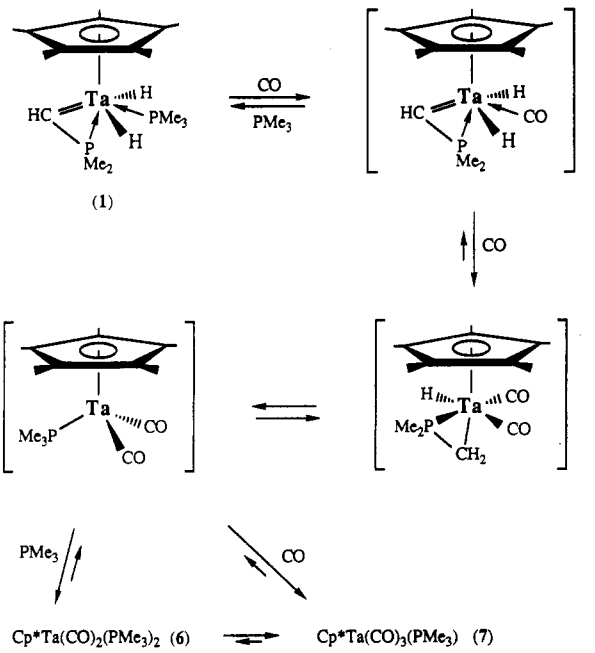

(3) Tolman, C. A. *Chem. Rev.* **1977**, *77*, 313.
(4) Pearson, R. G. *Chem. Brit.* **1967**, *3*, 103.
(5) (a) Gibson, V. C.; Graimann, C. E.; Hare, P. M.; Green, M. L. H.; Bandy, J. A.; Grebenik, P. D.; Prout, K. *J. Chem. Soc., Dalton Trans.* **1985**, 2025. (b) Green, M. L. H.; Hare, P. M.; Bandy, J. A. *J. Organomet. Chem.* **1987**, *330*, 61.

(6) (a) Mayer, J. M.; Bercaw, J. E. *J. Am. Chem. Soc.* **1982**, *104*, 2157. (b) Gibson, V. C.; Kee, T. P.; Clegg, W. *J. Chem. Soc., Dalton Trans.* **1990**, 3199.

time, since, in the presence of excess carbon monoxide, **6** converts slowly to **7** at room temperature with release of PMe_3.[6b] Signals attributable to C_5Me_5 and coordinated and free PMe_3 only are observed in the ^1H NMR spectrum, confirming that the classical PMe_3 group is regenerated from the $[M(H)_2(\eta^2\text{-}CHPMe_2)]$ moiety. The rate of the reaction is also inhibited by excess PMe_3, suggesting that PMe_3 displacement from **1** is rate limiting. Scheme II outlines a mechanistic pathway that is consistent with these observations.

The d^0 monocarbonyl adduct is related to $[Cp^*_2ZrH_2(CO)]$[7] and would not be expected to be long-lived under the reaction conditions. Migration of a hydride ligand to the metallacycle carbon will give a Ta(III) species that may be trapped by CO. Coordination of two CO ligands would then afford an 18-electron species analogous to the dmpe adduct **5**. A further hydride → metallacycle carbon migration is then required to regenerate the PMe_3 ligand, and trapping of the resultant $[Cp^*Ta(CO)_2(PMe_3)]$ species would account for the observation of both **6** and **7**.

Treatment of **1** with ca. 4 atm of dihydrogen in a sealed NMR tube shows a quantitative conversion to $Cp^*Ta(PMe_3)_2H_4$ (**8**), which has been characterized by comparison with data from an authentic sample.[6a]

4. Reactions of 1 with MeX (X = Cl, Br, I). (i) Preparation of $Cp^*Ta(PMe_3)(H)(X)(\eta^2\text{-}CHPMe_2)$ Complexes. **1** reacts with unimolar equivalents of methyl bromide and methyl iodide at room temperature to give the colorless, crystalline hydrido–halide complexes **9a** and **9b** in good yield, as shown in Scheme I. The reaction of **1** with methyl chloride gave a mixture of starting material and two products, the major component of which is **9c**. This derivative has been characterized by NMR spectroscopy only, which, in all cases, clearly shows that the $Ta(CHPMe_2)$ metallacycle is retained in the products. The resonance attributable to the methyl hydrogens of the bound PMe_3 ligand is relatively broad at room temperature and broadens further upon warming, suggesting that the PMe_3 ligand is somewhat more labile than for **1**. This is not unreasonable due to the greater steric demand of the halide over hydride ligand and the reduced metal acidity in **9a–c** due to X → M $p\pi$–$d\pi$ donation. A similar explanation has been offered for the more facile PMe_3 dissociation in $Cp^*Ta(PMe_3)_2ClH_3$ relative to $Cp^*Ta(PMe_3)_2H_4$.[6a] Accordingly, values of K_p determined for the equilibrium between **9a,b** and PMe_2Ph are smaller (4.3 (3) $\times 10^{-2}$ (**9a**), 2.7 (3) $\times 10^{-2}$ (**9b**)) than those found between **1** and **3a**.

(ii) Preparation of $(\eta\text{-}C_5Me_5)Ta(\eta^2\text{-}CHPMe_2)X_2$ (X = Cl, Br, I). The reaction of **1** with excess methyl bromide or methyl iodide in toluene proceeds cleanly via the monohalide complexes **9a** and **9b** to give the dihalide compounds **11a** and **11b**, respectively (Scheme I). The dichloride derivative **11c** is also accessible via the reaction of **1** with excess methyl chloride; this derivative has been characterized by NMR spectroscopy only.

Introduction of the second halide ligand results in elimination of PMe_3 from the metal coordination sphere, which combines with MeX to give $[Me_4P]^+X^-$ as a by-product. It is presumed that substitution of the second halide renders the metal center sterically and electronically reluctant to coordinate a PMe_3 ligand. However, the dihalide complexes do interact weakly with PMe_3 in solution, as indicated by a small downfield shift in the PMe_3 methyl resonance of the phosphine when in contact with benzene-d_6 solutions of **11a–c**.

(7) Wolczanski, P. T.; Bercaw, J. E. *Acc. Chem. Res.* **1980**, *13*, 121.

The spectroscopic data for **11a–c** support a monomeric formulation analogous to the isoelectric compounds $Cp^*Ta(\eta^2\text{-}RC{\equiv}CR)X_2$ (R = Me, Ph, H).[8] The presence of the $(\eta^2\text{-}CHPMe_2)$ metallacycle is confirmed by characteristic shifts in the NMR spectrum, and the equivalence of the PMe_2 methyls suggests that a plane of symmetry is present which contains the carbon and phosphorus atoms of the metallacycle. Difference nOe experiments confirm that the $CHPMe_2$ ligand is orientated the same way around, i.e. with the CH end toward the Cp* ring, as in the parent compound **1**.

Nature of the η^2-$CHPMe_2$ Ligand. The bond lengths found in the $Ta(\eta^2\text{-}CHPMe_2)$ metallacycle are consistent with a contribution to the metal–ligand bonding from canonical forms I and II.[2a,c] I may be regarded as a

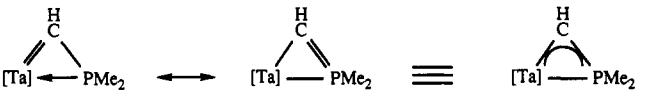

I II III

phosphinocarbene contributing 4 electrons to the metal ligand bonding, while II is a λ^5-phosphacetylene and is closely related to the metallacyclopropene bonding form of an acetylene ligand. Which of these localized bonding forms is a more appropriate representation is difficult to discern from spectroscopic and reactivity studies.[2c] However, the similarities between **11** and previously characterized $Cp^*TaCl_2(\eta^2\text{-}RC{\equiv}CR)$[8] (**12**) presented an opportunity to compare the acetylene ligand with η^2-$CHPMe_2$ and to learn more about the nature of the metal–ligand interactions for the latter.

The first point to note from the crystal structures of **1** and **12** is that the orientations of the η^2-$CHPMe_2$ and η^2-$RC{\equiv}CR$ ligands with respect to the $[Cp^*TaCl_2]$ fragment are quite different: the C–C multiple bond of the acetylene lies parallel to the plane of the C_5Me_5 ring, while the corresponding C–P multiple bond is orientated perpendicular. Fenske–Hall quantum chemical calculations[9] have been carried out on the model systems $(\eta\text{-}C_5Me_5)NbCl_2(\eta^2\text{-}HC{\equiv}CH)$ (**13**) and $(\eta\text{-}C_5Me_5)NbCl_2(\eta^2\text{-}CHPMe_2)$ (**14**) by using the geometries based on the crystal structures of **1**[2a,c] and $(\eta\text{-}C_5Me_5)TaCl_2(\eta^2\text{-}PhC{\equiv}CPh)$.[8]

$(\eta\text{-}C_5Me_5)NbCl_2$ Fragment. The frontier orbitals of the $(\eta\text{-}C_5Me_5)NbCl_2$ fragment are represented schematically on the left-hand side of Figure 1. Before discussing the interaction of these orbitals with those of the HCCH or $HCPMe_2$ ligands, it is important to note their orientations with respect to the interfragment axis (defined as the x axis in **13** and **14**). The unoccupied MO 40 tilts slightly

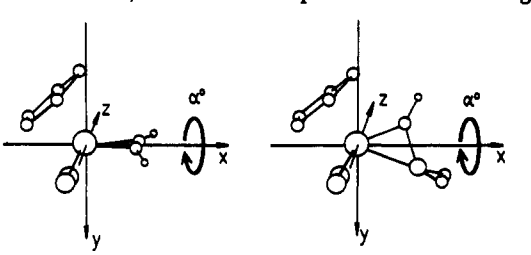

13 **14**

above the x axis and MO 39 points significantly down. The HOMO and LUMO (MO's 37 and 38) both contain negative y components.

(8) Smith, G.; Schrock, R. R.; Churchill, M. R.; Youngs, W. J. *Inorg. Chem.* **1981**, *20*, 387.
(9) Hall, M. B.; Fenske, R. F. *Inorg. Chem.* **1972**, *11*, 768.

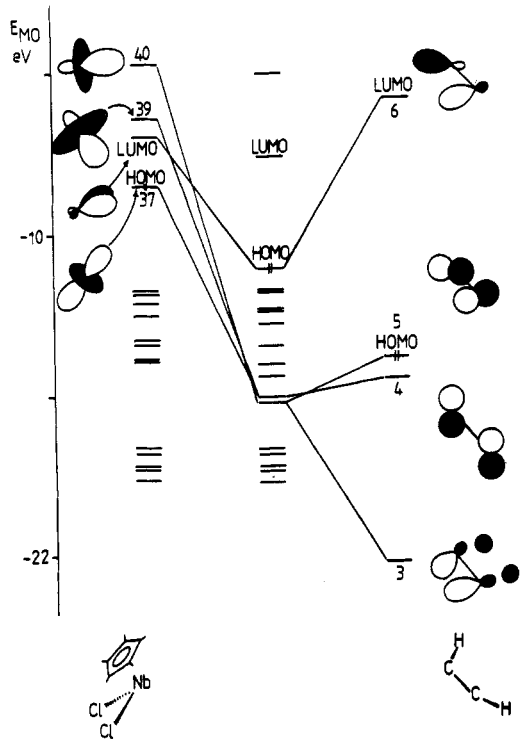

Figure 1. Orbital correlation diagram for the interaction of the $(\eta^5\text{-}C_5Me_5)NbCl_2$ and HCCH fragments, with $\alpha = 0°$, and schematic representations of the frontier molecular orbitals of the fragments. The fragment MO energies are taken from the Fock matrix of the complex.[11]

Interaction of the $(\eta\text{-}C_5Me_5)NbCl_2$ and HCCH Fragments ($\alpha = 0°$) To Generate 13. The formation of **13** from the $(\eta\text{-}C_5Me_5)NbCl_2$ and HC≡CH fragments may be envisaged quite simply as shown in Figure 1. In terms of interfragment Mulliken overlap populations, the two most important interactions are those between MO's 38 and 6,[10] and 40 and 5; 48% and 26%, respectively, of the total net Mulliken overlap population may be attributed to these interactions. The ability of MO's 37 and 39 of the $(\eta\text{-}C_5Me_5)NbCl_2$ fragment to interact with the acetylene π orbital, MO 4, is critically dependent upon the deviation of the metal 4d hybrid orbital from the x axis, a point that we shall address further below.

Interaction of the $(\eta\text{-}C_5Me_5)NbCl_2$ and $HCPMe_2$ Fragments ($\alpha = 90°$) To Generate 14. Using a set of valence orbitals for the P atom restricted to 3s and 3p AO's leads to frontier orbitals for the $HCPMe_2$ fragment, as shown on the right-hand side of Figure 2. The asymmetry of the ligand is naturally reflected in the composition of the MO's, and in particular, MO 12 is seen to be predominantly localized on the carbon atom. The major orbital interactions of the ligand with the $(\eta\text{-}C_5Me_5)NbCl_2$ fragment to generate **14** are summarized in Figure 2. Interfragment Mulliken overlap populations for the MO interactions 38–12, and 37–13 account for 26% and 27%, respectively, of the total overlap population, with 15% due to the interaction 39–13 and 13% due to the interaction 40–11. As in the case of the formation of the complex **13**, the orientation of MO 37 of the metal fragment is crucial to its effective overlap with the P–C antibonding orbital, MO 13 (Figure 3a). The interaction of MO's 38 and 12,

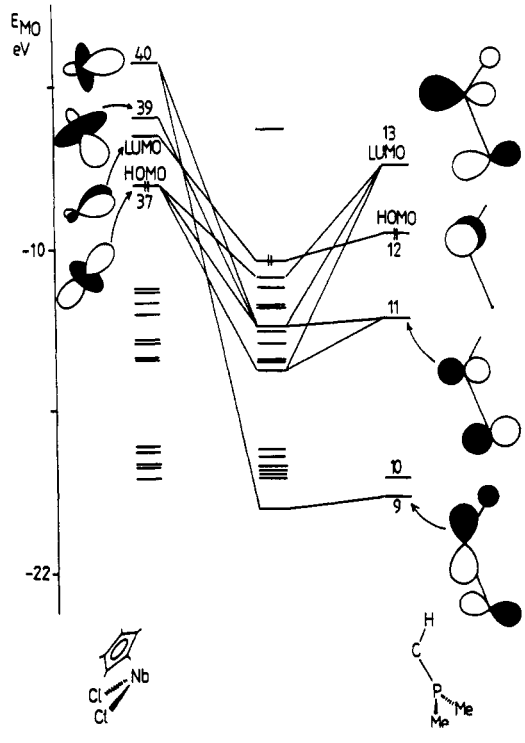

Figure 2. Orbital correlation diagram for the interaction of the $(\eta^5\text{-}C_5Me_5)NbCl_2$ and $HCPMe_2$ fragments, with $\alpha = +90°$, and schematic representations of the frontier molecular orbitals of the fragments, allowing a P atom AO basis set restricted to 3s and 3p orbitals. The fragment MO energies are taken from the Fock matrix of the complex.[11]

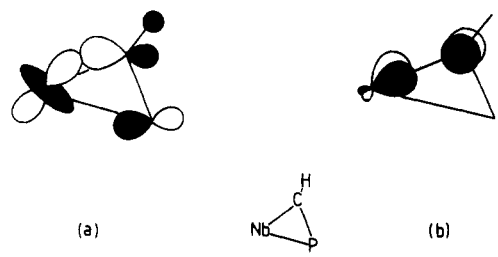

Figure 3. Schematic representations of the interactions between (a) MO's 37 and 13 and (b) MO's 38 and 12 of the $(\eta^5\text{-}C_5Me_5)NbCl_2$ and $HCPMe_2$ fragments, respectively.

shown schematically in Figure 3b, generates an effective Nb–C bond of localized[12] π symmetry. The significant contribution made by this interaction to the net interfragment bonding may be interpreted in terms of the ligand functioning as a phosphinocarbene. This is in keeping with the results of an ab initio study on the free $HCPH_2$.[13]

The inclusion of a set of 3d AO's in the orbital basis set of the phosphorus atom leads to only minor perturbations of the bonding description above. Of the frontier orbitals of the $HCPMe_2$ fragment, MO's 12 and 13 pick up 3d character; MO 12 (HOMO) is stabilized by ≈1.4 eV, while MO's 11 and 13 are each stabilized by ≈0.3 eV. Since the symmetries of the ligand MO's do not alter, the major interfragment interactions remain as depicted in Figure 2, although the character of the interactions is spread through eight, rather than five, MO's of **14**. One feature worth noting is that, while the contribution made to the net bonding by the interaction of MO's 38–12 remains unaltered, the availability of phosphorus 3d orbitals does

(10) Note that interaction between two unoccupied MO's is allowed, since our criteria for efficient overlap are compatible orbital symmetries and energies; the same phenomenon has been observed in related systems.[11]

(11) Kostic, N. M.; Fenske, R. F. *Inorg. Chem.* **1983**, *22*, 666.

(12) Localized with respect to the Nb–C vector.

(13) Nguyen, M. T.; McGinn, M. A.; Hegarty, A. F. *Inorg. Chem.* **1986**, *25*, 2185.

introduce ca. 10% P character into the complex MO we previously assigned as being "carbene-like". Finally, the total interfragment Mulliken overlap population is 0.609 electrons (compared to 0.601 e^- in the absence of P atom 3d AO's), and the net transfer of charge is 0.27 e^- from metal → ligand (compared to 0.20 e^- when 3d AO's are not available). Hence, we conclude that, within the constraints of the Fenske–Hall approach, the participation of the phosphorus 3d orbitals in the bonding of the $HCPMe_2$ ligand to the (η-C_5Me_5)$NbCl_2$ fragment is not significant.

Interaction of the (η-C_5Me_5)$NbCl_2$ and HCCH or $HCPMe_2$ Fragments as a Function of Angle α. The crystallographically observed geometry for the acetylene ligand in the complex (η-C_5Me_5)$TaCl_2$(PhC≡CPh) is one that places the C–C vector parallel to the C_5Me_5 ring (i.e. α = 0°). This orientation is expected on steric grounds for the diphenylacetylene ligand and is also anticipated for other alkynes.[8] However, an exception exists; the benzyne ligand in the complex (η-C_5Me_5)$TaCl_2(C_6H_4)$ exhibits a "perpendicular" (i.e. α = 90°) orientation.[14] This has been rationalized in terms of maximizing the interaction of the metal fragment with the benzyne ring π-electron cloud.[8] In view of our observation that the $HCPMe_2$ ligand binds in a perpendicular mode in (η-C_5Me_5)$TaCl_2(\eta^2$-$CHPMe_2$) and, moreover, specifically in an orientation that places the PMe_2 group on the same side of the metal as the two chlorine atoms, we decided to investigate more closely the effects on the electronic structure of the complexes **13** and **14** of rotating the acetylene-type ligands, while keeping the metal fragment in a fixed position.

Rotation of the HCCH ligand in complex **13** between the limits α = 0–90° explores all possible orientations for this symmetrical ligand. The interaction of the (η-C_5Me_5)$NbCl_2$ and HCCH fragment MO's 38 and 6 will be effective for α = 0° but disallowed by symmetry for α = 90°. The reverse is true for overlap between MO's 38 and 4. Similarly, rotation of the ligand from α = 0 to 90° "turns on" the interactions 37–6 and 39–6 and "turns off" the interactions 37–4 and 39–4 (Figure 4). However, the total change in interfragment Mulliken overlap population for the MO 37/38/39–4/6 interactions is small; only a 6% net decrease is observed in going from α = 0 to 90°.

Let us now consider interactions of the ligand MO's with MO 40 of the (η-C_5Me_5)$NbCl_2$ fragment. The orbital is of a_1 symmetry and is thus compatible with the a_1 (π-bonding) orbital and the lower lying orbital MO 3 (derived from carbon sp hybrids) of the acetylene ligand. However, MO 40 does not point directly at the center of the alkyne's C–C bond. Thus, the interactions between MO's 40 and 3, or 5, are dependent upon α. The overlap 40–3 is negligible, but overlap 40–5 is significant, and there is a 23% decrease in the overlap population in going from α = 0 to 90°, as shown in Figure 4.

The overall picture in going from a parallel to a perpendicular geometry for the acetylene ligand is one of decreasing interfragment overlap, but in terms of electronic effects, the preference for the parallel orientation is fairly marginal. Thus, we might expect the balance to be easily tipped by steric effects (i.e. bulky substituents will favor the parallel position).

Consider now the phosphinocarbene ligand. Since it is inherently asymmetrical, rotation angles of α = 0 to ±90° must be investigated (note that the experimentally observed ligand orientation has α = +90°). A graph corresponding to Figure 4 may be constructed, showing orbital

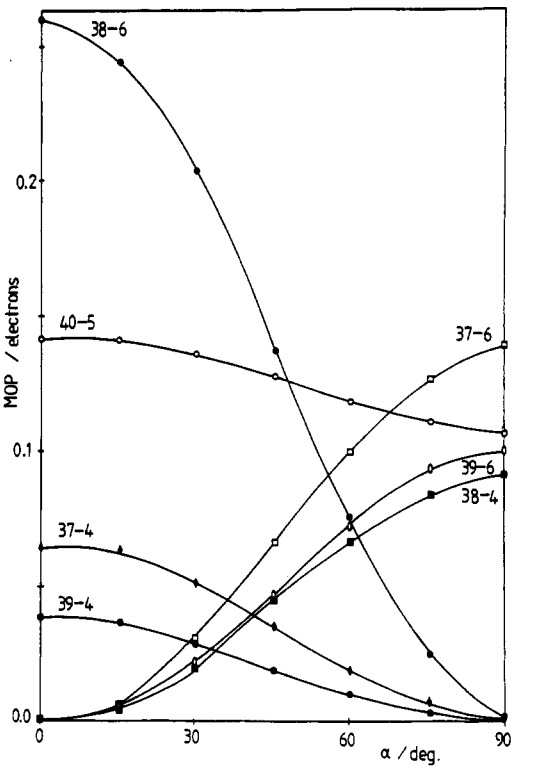

Figure 4. Major orbital interactions between the (η^5-C_5Me_5)$NbCl_2$ and HCCH fragments as a function of the rotation angle, α. MOP = Mulliken overlap population.

interactions clearly related to those operating in complex **13**. However, unlike the competition described above for orbital interactions in **13**, in complex **14** the total Mulliken overlap population between MO's 37, 38, and 39 of the (η-C_5Me_5)$NbCl_2$ fragment and MO's 12 and 13 of the $HCPMe_2$ fragment for α = +90° is greater than that either at α = 0° or −90°, viz. 0.408 vs 0.381 or 0.342 electrons, respectively.

The participation of the a_1 orbital of the (η-C_5Me_5)$NbCl_2$ fragment in forming **14** follows the trend observed in complex **13**. The interaction between MO's 40 and 11 is rendered most effective at α = 0° rather than α = ±90°; there is a 40% increase in the overlap population of MO 40 with the ligand MO 11 in going from a perpendicular to the parallel orientation. This preference must therefore compete against that dictated by the interfragment interactions of π-type symmetry outlined above. The overall result, aided by several minor interactions, is a summed interfragment Mulliken overlap population of 0.559, 0.536, and 0.527 e^- for α = +90, 0, and −90°, respectively. Again, the balance is a fine one and is perhaps swung in favor of α = +90° by the stabilization of the HOMO in **14**; the HOMO–LUMO gap[15] alters as a function of the rotation angle, being ≈4.8 eV for α = +90° and ≈4.1 and ≈3.9 eV for α = 0 and −90°, respectively. In addition, metal → ligand back-bonding is most effective when the $HCPMe_2$ moiety is in the perpendicular orientation; the net gain in electronic charge is 0.20, 0.13, and 0.19 e^- for α = +90, 0, and −90°, respectively.

Summary

Although hydrogen migrations to the [Ta(CHPMe$_2$)] metallacycle carbon are too slow to be observed conven-

(14) Churchill, M. R.; Youngs, W. J. *Inorg. Chem.* **1979**, *18*, 1697.

(15) Absolute values for the HOMO–LUMO energy gap are a function of the experimental method; we expect the trend, but not the values, to be reproduced by other methods.

iently by NMR spectroscopy, the reactions of **1** with dmpe and carbon monoxide establish that such migrations do occur on the time scale of a chemical reaction. In the absence of hydride ligands, the [Ta(CHPMe$_2$)] unit appears to be quite robust, suggesting that a substantial derivative chemistry of species containing this ligand should prove accessible through compounds such as the mono- and dihalides **9** and **11**.

The calculations suggest that the most appropriate *localized* bonding picture for the CHPMe$_2$ ligand is a phosphinocarbene form in which the ligand contributes 4 electrons to the metal center, two via σ- and π-covalent interactions with carbon and two via a phosphorus-to-metal lone-pair donation. It is worth noting that these bonding components are reminiscent of metal–imido (M≡NR) interactions, and therefore, similarities between the derivative chemistry of Cp*Ta(η^2-CHPMe$_2$)X$_2$ (X = halide, hydride, alkyl, etc.) and their imido analogues Cp*Ta(NR)X$_2$[16] may be anticipated. Moreover, since the CHPMe$_2$ group formally contributes one electron less than a neutral η^5-C$_5$R$_5$ ligand, a relationship is also apparent between Cp*Ta(η^2-CHPMe$_2$)X$_2$ and the group 4 bent metallocenes of the type CpCp'MX$_2$ (M = Ti, Zr, Hf). Future studies will attempt to evaluate these relationships.

Experimental Section

General Methods. All manipulations of air- and/or moisture-sensitive materials were performed on a conventional vacuum/inert-atmosphere (nitrogen or argon) line by using standard Schlenk and cannula techniques or in an inert-atmosphere nitrogen- or argon-filled drybox.

The following solvents were dried by prolonged reflux over a suitable drying agent and were freshly distilled and deoxygenated prior to use (drying agent in parentheses): toluene (sodium metal), petroleum ether (bp 40–60 °C, lithium aluminum hydride), petroleum ether (bp 100–120 °C, sodium metal), and tetrahydrofuran (sodium benzophenone ketyl). Benzene-d_6 and toluene-d_8 were dried by vacuum distillation from phosphorus(V) oxide and stored over activated 4-Å molecular sieves.

Elemental analyses were performed by the microanalytical services of this department. Infrared spectra were recorded on Perkin-Elmer 577 and 457 grating spectrophotometers by using either KBr or CsI windows. Absorptions are abbreviated as s (strong), m (medium), w (weak), br (broad), sp (sharp), and sh (shoulder). Mass spectra were recorded on a VG 7070E mass spectrometer. NMR spectra were recorded on the following instruments, at the frequencies listed, unless stated otherwise: Bruker AC 250, ^{1}H (250.13 MHz), ^{13}C (62.90 MHz), ^{31}P (101.26 MHz). The following abbreviations have been used for band multiplicities: s (singlet), d (doublet), t (triplet), q (quartet), qnt (quintet), m (multiplet). Chemical shifts are quoted to the following references, unless stated otherwise: ^{31}P (dilute aqueous H$_3$PO$_4$, 0 ppm); ^{13}C (C$_6$D$_6$, 128.0 ppm); ^{1}H (C$_6$D$_6$, 7.15 ppm).

The following chemicals were prepared by previously published procedures: PMe$_3$,[5a] Cp*TaCl$_4$,[17] Cp*H,[18] and Bu$^n_3$SnCp*.[19] All other chemicals were obtained commercially and used as received unless stated otherwise.

Cp*Ta(dmpe)(H)(η^2-CHPMe$_2$) (5). Dmpe (0.19 g, 1.28 mmol) was added via syringe to a toluene solution (30 mL) of Cp*Ta(PMe$_3$)(H)$_2$(η^2-CHPMe$_2$) (0.6 g, 1.28 mmol) in an argon-filled drybox. The mixture was heated at 70 °C for 3 h to afford an orange solution. The volatile components were then removed under reduced pressure, and the residue was extracted into light petroleum ether (50 mL). Filtration, followed by concentration to ca. 8–10 mL and cooling to −78 °C afforded orange crystals, which were collected and dried in vacuo. Yield: 0.47 g, 68%. Anal. Calcd for C$_{19}$H$_{40}$P$_3$Ta: C 42.06; H 7.45. Found: C 42.02; H 7.51. Mass spectrum (EI, 70 eV): *m/e* 542 ([M]$^+$), 464 ([M − PMe$_3$ − 2H]$^+$). IR (cm^{-1}, CsI, Nujol): 1650 (m, br), 1422 (m), 1292 (m), 1275 (m), 1265 (m), 1100 (w, br), 1030 (m), 938 (s, br), 918 (m, sh), 893 (m), 825 (m), 800 (m), 715 (m), 705 (m), 680 (m), 667 (m), 615 (m), 460 (w), 425 (w), 396 (m), 350 (m, br).

Cp*Ta(PMe$_3$)(H)(Br)(η^2-CHPMe$_2$) (9a). Methyl bromide (0.81 g, 8.55 mmol) was condensed from a graduated "cold-finger" onto a frozen solution of Cp*Ta(PMe$_3$)(H)$_2$(η^2-CHPMe$_2$) (0.8 g, 1.71 mmol) in toluene (40 mL) in a 150-mL "rotoflo" glass ampule. Upon warming of the solution to ca. −20 °C, nitrogen was admitted and stirring was maintained at room temperature for 3 h. The solution was then filtered, and the volatiles were removed under reduced pressure. The off-white crystalline product was recrystallized from light petroleum ether (35 mL) at −78 °C to afford colorless crystals, which were dried in vacuo. Yield: 0.82 g, 88%. Anal. Calcd for C$_{16}$H$_{32}$BrP$_2$Ta: C 35.08; H 5.91. Found: C 35.47; H 6.02. Mass spectrum (EI, 70 eV): *m/e* 470 ([M − PMe$_3$ − H]$^+$), 394 ([M − 2PMe$_3$ − H]$^+$). IR (cm^{-1}, KBr, Nujol): 3100 (w), 1710 (m, br), 1420 (m), 1300 (m, sp), 1280 (m, sp), 1270 (m, sp), 1030 (w), 970 (s), 950 (s), 930 (m), 895 (w), 890 (w), 885 (w), 860 (w), 730 (m), 725 (m), 690 (m), 670 (w), 650 (w), 625 (w), 600 (m).

Cp*Ta(PMe$_3$)(H)(I)(η^2-CHPMe$_2$) (9b). Methyl iodide (0.12 g, 0.85 mmol) was added via syringe to a solution of Cp*Ta(PMe$_3$)(H)$_2$(η^2-CHPMe$_2$) (0.4 g, 0.85 mmol) in toluene (25 mL) at room temperature in a nitrogen-filled drybox. The resulting solution was stirred for 24 h at room temperature, filtered, concentrated to ca. 5 mL, and cooled to −78 °C to afford colorless crystals, which were collected, washed with light petroleum ether (5 mL), and dried in vacuo. Yield: 0.35 g, 69%. Anal. Calcd for C$_{16}$H$_{32}$IP$_2$Ta: C 32.33; H 5.44. Found: C 32.21; H 5.48. Mass spectrum (CI, isobutane): *m/e* 518 ([M − PMe$_3$]$^+$), 442 ([M − 2PMe$_3$]$^+$). IR (cm^{-1}, KBr, Nujol): 1755 (m, br), 1730 (m, br), 1415 (m), 1300 (m, sp), 1280 (s, sp), 1273 (m, sh), 1160 (w), 1072 (w), 1030 (m), 969 (s), 955 (s), 929 (s), 865 (w), 850 (w), 835 (w), 730 (s), 690 (m), 670 (w), 654 (w), 630 (m), 600 (m).

Cp*Ta(Br)$_2$(η^2-CHPMe$_2$) (11b). Methyl bromide (0.5 g, 5.3 mmol) was condensed onto a frozen solution of Cp*Ta(PMe$_3$)(H)$_2$(η^2-CHPMe$_2$) (0.25 g, 0.53 mmol) in toluene (25 mL). Upon warming of the solution to room temperature, nitrogen was admitted and the reaction mixture was heated to 70 °C for 4 h to give a dark red-brown solution over a pale precipitate. The supernatant solution was removed by filtration and the residue washed with toluene (2 × 10 mL). The combined toluene extracts were concentrated (10 mL) and layered with light petroleum ether (20 mL). The resultant orange crystals were collected, washed with light petroleum ether (2 × 5 mL), and dried in vacuo. Yield: 0.19 g, 65%. Anal. Calcd for C$_{13}$H$_{22}$Br$_2$PTa: C 28.38; H, 4.04. Found: C 28.54; H 4.12. Mass spectrum (CI, isobutane): *m/e* 551 ([M + H]$^+$), 471 ([M − Br + H]$^+$). IR (cm^{-1}, KBr, Nujol): 1420 (m), 1282 (m), 1075 (w), 1030 (m), 955 (s, br), 869 (m), 840 (w), 740 (m), 703 (m), 665 (m).

Cp*Ta(I)$_2$(η^2-CHPMe$_2$) (11c). Methyl iodide (0.61 g, 4.3 mmol) was added via syringe to a stirred solution of Cp*Ta(PMe$_3$)(H)$_2$(η^2-CHPMe$_2$) (0.4 g, 0.85 mmol) in toluene (30 mL) at room temperature. After the dark solution was stirred for 4 days, it was filtered, and the remaining pale residue was washed with toluene (2 × 10 mL). The combined toluene extracts were concentrated to ca. 10 mL and layered with light petroleum ether (20 mL) to give orange-brown microcrystals, which were washed with light petroleum ether (2 × 5 mL) and dried in vacuo. Yield: 0.43 g, 78%. Anal. Calcd for C$_{13}$H$_{22}$I$_2$PTa: C 24.24; H 3.45. Found: C 23.76; H 3.37. Mass spectrum (CI, isobutane): *m/e* 645 ([M − H]$^+$), 517 ([M − I]$^+$). IR (cm^{-1}, CsI, Nujol): 1415 (m, br), 1295 (m), 1287 (m), 1075 (m), 1064 (m), 1021 (m), 962 (s, br), 881 (m), 865 (m), 783 (w), 762 (m), 754 (m), 730 (m), 693 (w), 580 (w), 365 (s), 312 (w).

Calculations. The Fenske–Hall quantum chemical calculations[9] were carried out on the model systems (η-C$_5$Me$_5$)NbCl$_2$(η^2-HC≡CH) (**13**) and (η-C$_5$Me$_5$)NbCl$_2$(η^2-CHPMe$_2$) (**14**) by using the geometries based on the crystal structures of **1**[2a,c] and (η-C$_5$Me$_5$)TaCl$_2$(η^2-PhC≡CPh).[8] Bond distances used in the calculations were Nb–Cl = 2.56, Nb–C(Cp*) = 2.42, Nb–C(HCCH) = 2.07, C–C(HCCH) = 1.33, Nb–P = 2.48, Nb–C(CHPMe$_2$) = 2.00, and P–C = 1.71 Å. The geometry of the (η-C$_5$Me$_5$)NbCl$_2$ fragment

(16) Mitchell, J. P.; Gibson, V. C. Unpublished results.
(17) Gibson, V. C.; Bercaw, J. E.; Bruton, W. J., Jr.; Sanner, R. D. *Organometallics* **1986**, *5*, 976.
(18) Manriquez, J. M.; Fagan, P. J.; Schertz, L. D.; Marks, T. J. *Inorg. Synth.* **1982**, *21*, 181.
(19) Sanner, R. D.; Carter, S. T.; Bruton, W. J., Jr. *J. Organomet. Chem.* **1982**, *240*, 157.

(common to both complexes 13 and 14) was idealized to C_s symmetry. Each of the HCCH and $HCPMe_2$ ligands was rotated through $\alpha°$, about the x axis, which passes through the metal atom and the C–C, or P–C bond, so as to maintain constant Nb–C, or Nb–P, distances. For $\alpha = 0°$, the acetylene or phosphaacetylene ligand lies parallel to the C_5Me_5 ring. Thus, in 13, $\alpha = 0°$, while, in 14, $\alpha = +90°$. The role of the phosphorus 3d orbitals was tested by comparing the results of calculations in which the atomic orbital basis set of the P atom was restricted to valence 3s and 3p and then was expanded to include 3d orbitals.

The Fenske–Hall calculations employed single-ζ Slater functions for the 1s and 2s functions of C, P, and Cl. The exponents were obtained by curve fitting the double-ζ functions of Clementi[20] while orthogonal functions were maintained; the double-ζ functions were used directly for the 2p orbitals. For P, an expanded atomic orbital basis set used an exponent for the 3d functions of 1.80. An exponent of 1.16 was used for hydrogen. The Nb functions,[21] chosen for the +1 oxidation state, were augmented by 5s and 5p functions with exponents of 2.20.

Acknowledgment. V.C.G. wishes to thank the SERC for a research grant and a studentship (to T.P.K.). C.E.H. gratefully acknowledges the award of a 1983 University Research Fellowship by the Royal Society. H.M.A. thanks the laboratory of the Government Chemist for undergraduate sponsorship. We are also grateful to Dr. D. Reed for advice and help with high-field NMR experiments.

(20) Clementi, E. *J. Chem. Phys.* **1964**, *40*, 1944.

(21) Richardson, J. W.; Blackman, M. J.; Ranochak, J. E. *J. Chem. Phys.* **1973**, *58*, 3010.

1-Sila-3-metallacyclobutanes, Precursors for the Generation of Highly Electrophilic Group 4 Metallocene Alkyl Cations. Spectroscopic and Structural Evidence of a Weakly Bound THF Ligand in $[(C_5Me_5)_2Zr(CH_2SiMe_3)(THF)][BPh_4]$

David M. Amorose, Rip A. Lee, and Jeffrey L. Petersen*

Department of Chemistry, West Virginia University, Morgantown, West Virginia 26506-6045

Received December 7, 1990

The protonation of $L_nM(CH_2SiMe_2CH_2)$ ($L_n = (C_5H_5)_2$, $SiMe_2(C_5H_4)_2$ M = Ti, Zr; $L_n = (C_5Me_5)_2$ M = Zr) with $[NEt_3H][BPh_4]$ in THF produces the corresponding (trimethylsilyl)methyl-substituted metal alkyl tetraphenylborate salts $[L_nM(CH_2SiMe_3)(THF)][BPh_4]$ (1–5). These complexes have been characterized by elemental analysis and ^1H and ^{13}C NMR measurements. The molecular structure of $[Cp^*_2Zr(CH_2SiMe_3)(THF)][BPh_4]$ (5) has been determined by X-ray diffraction methods. Complex 5 crystallizes in space group $P2_1/a$ with $a = 26.911$ (9) Å, $b = 13.929$ (4) Å, $c = 12.569$ (4) Å, $\beta = 101.73$ (2)°, $V = 4613$ (3) Å^3, and $Z = 4$. The steric bulk of the pentamethylcyclopentadienyl ligands controls the orientation of the THF molecule, placing it nearly "parallel" to the equatorial plane of the metallocene wedge. Attempts to prepare the THF-free cation $[Cp^*_2Zr(CH_2SiMe_3)]^+$ by the reaction of $Cp^*_2Zr(CH_2SiMe_2CH_2)$ with $[N(n\text{-butyl})_3H][BPh_4]$ in toluene led to the isolation of the previously reported zwitterion $Cp^*_2Zr(+)\text{-}(m\text{-}C_6H_4)\text{-}B(-)Ph_3$ (6). Compounds 1–4 (in CH_2Cl_2) and compound 6 (in toluene) behave as ethylene polymerization catalysts, producing high-density polyethylene (HDPE) under mild conditions in the absence of an Al cocatalyst.

Introduction

Bis(cyclopentadienyl)metal complexes such as Cp_2MCl_2 (M = Ti, Zr) in the presence of aluminum alkyl reagents constitute an important class of soluble catalysts for Ziegler–Natta olefin polymerization.[1] Although initial efforts by Shilov and co-workers[2] to identify the catalytically active species were unsuccessful, they suggested that the polymerization process involves the participation of a highly electrophilic, cationic metallocene alkyl complex, Cp_2MR^+. Indirect evidence of its existence was provided by Eisch and co-workers,[3] who trapped and structurally characterized the cationic alkenyl species $[Cp_2Ti(C(SiMe_3)=C(Ph)Me)][AlCl_4]$, following the addition of $PhC{\equiv}CSiMe_3$ to an active catalyst mixture containing titanocene dichloride and $AlMeCl_2$. Although the isolation of Cp_2TiMe^+ and related d^0, $14e^-$ cations remains to be accomplished, several different synthetic strategies have been employed to prepare THF adducts of these species. Taube and Krukowka[4] have reported that $[Cp_2TiMe(THF)][BPh_4]$ is obtained by partial protonolysis of Cp_2TiMe_2 by $[NPhMe_2H][BPh_4]$ in a CH_2Cl_2/THF mixture. Similar strategies were employed by Marks and co-workers[5] to prepare a variety of cationic organothorium compounds, including $[Cp^*_2ThMe(THF)_2][BPh_4]$, and by Teuben and co-workers[6] for the preparation of $[Cp^*_2MMe(THT)][BPh_4]$, where M = Ti, Zr, Hf and THT

(1) (a) Natta, G.; Pino, P.; Mazzanti, G.; Giannini, U. *J. Inorg. Nucl. Chem.* **1958**, *18*, 612. (b) Breslow, D. S.; Newburg, N. R. *J. Am. Chem. Soc.* **1959**, *81*, 81. (c) Ziegler, K.; Gellert, H. G.; Zosel, K.; Holzkamp, E.; Schneider, J.; Soll, M.; Kroll, W. R. *Justus Liebigs Ann. Chem.* **1960**, *629*, 121. (d) Sinn, H.; Kolk, E. *J. Organomet. Chem.* **1966**, *6*, 373. (e) Sinn, H.; Kaminsky, W. *Adv. Organomet. Chem.* **1980**, *18*, 99.

(2) Dyachkovskii, F. S.; Shilova, A. K.; Shilov, A. E. *J. Polym. Sci., Part C* **1967**, *16*, 2333.

(3) Eisch, J. J.; Piotrowski, A. M.; Brownstein, S. K.; Gabe, E. J.; Lee, F. L. *J. Am. Chem. Soc.* **1985**, *107*, 7219.

(4) Taube, R.; Krukowka, L. *J. Organomet. Chem.* **1988**, *C9*, 347.

(5) Lin, Z.; Le Marechal, J.-F.; Sabat, M.; Marks, T. J. *J. Am. Chem. Soc.* **1987**, *109*, 4127.

(6) Eshuis, J. J. W.; Tan, Y. Y.; Teuben, J. H.; Renkema, J. *J. Mol. Catal.* **1990**, *62*, 277.

0276-7333/91/2310-2191$02.50/0